Light-scattering study of the localization of longitudinal acoustic pseudomodes in a buried silica layer

G. Ghislotti,* C.E. Bottani,* and P. Mutti
Dipartimento di Ingegneria Nucleare del Politecnico di Milano, Via Ponzio, 34/3, 20133 Milano, Italy

C. Byloos, L. Giovannini, and F. Nizzoli
Dipartimento di Fisica dell'Università di Ferrara, Via Paradiso, 12, 44100 Ferrara, Italy
and Istituto Nazionale di Fisica della Materia, Unità di Ricerca di Ferrara, Ferrara, Italy
(Received 29 November 1994)

Brillouin light spectroscopy in *p-p* backscattering geometry is used to study sagittal surface acoustic phonons in silicon on insulator structures formed on a silicon buffer. The experimental spectra show, near the longitudinal threshold of silicon, two peaks whose physical meaning is discussed by comparison with theoretical cross sections. Calculations of Brillouin cross sections were performed, taking into account both the ripple and elasto-optic coupling mechanisms. The peaks originate from two pseudomodes: the first is highly localized in the buried SiO_2 layer and the second in the top silicon layer. The dependence of the pseudomode localization and cross section intensity with the parallel wave vector and with the thickness of the top silicon layer are discussed.

I. INTRODUCTION

Brillouin light scattering has been extensively used to study the surface acoustic phonon power spectrum of opaque layered systems.[1] In these structures the phonon spectrum may exhibit, in addition to surface modes, very peculiar pseudomodes originating from quasiresonances in the continuum. In a film of ZnSe on GaAs, Hillebrands *et al.*[2] observed a pseudomode with a displacement field having longitudinal character and propagating in the film. Apart from its fundamental interest, the study of surface acoustic modes and pseudomodes by Brillouin spectroscopy has been used to characterize the elastic properties of films and superlattices.[3]

Recently, structures constituted by a SiO_2 layer buried in a silicon substrate, obtained by separation by oxygen implantation, have been studied by means of Brillouin light scattering. Silicon on insulator structures (SOI) are technologically interesting in view of their applications in microelectronics. From the acoustic point of view their interest is due to the presence of the buried silica layer, which can act as a waveguide since its sound velocity is lower than that of silicon. In *p-s* Brillouin spectra, guided modes and pseudomodes of shear horizontal polarization have been observed.[4,5] On the other hand, the *p-p* spectra show, in addition to the usual surface sagittal modes (Rayleigh and Sezawa waves), two pseudomodes of longitudinal polarization. These results have been presented in a preliminary paper,[6] where the longitudinal character of the pseudomodes has been identified. The first acoustic pseudomode having lower energy is localized in silica, while the second one is in the upper silicon layer. Although light may couple to both the dynamical corrugation of the surface (ripple effect) (Ref. 7) and the fluctuation of the dielectric function in the medium (elasto-optic effect), in the case of silicon on insulator structures only the elasto-optic mechanism is relevant for the two longitudinal pseudomodes.[6]

The present study is devoted to an extensive examination of these pseudomodes. For this purpose, we performed measurements at different incidence angles on samples having different thickness of the top silicon layer. Propagation along [100] and [110] directions were considered in order to decouple the sagittal and shear horizontal displacements. The results are compared with calculated theoretical cross sections. The details of the theory are presented elsewhere.[8]

II. EXPERIMENT

The examined SOI structures were prepared by oxygen implantation of (001)Si wafers and subsequent thermal annealing in an argon atmosphere in the temperature range 650–1350 °C. Samples having different thickness of the top silicon layer were prepared by thermal oxidation of the specimen surface and subsequent removal of the oxide layer by chemical etching. Samples were investigated by cross sectional transmission electron microscopy and present rather sharp interfaces. The thickness of the top silicon layer in the examined samples was 350, 250, and 150 nm, while that of the buried silica layer was 100 nm.

Brillouin spectra were acquired in backscattering geometry at room temperature, using a 3+3 passes tandem interferometer with an overall finesse of approximately 100.[9] Measurements were performed using incident *p*-polarized light from an argon-ion laser oscillating in single longitudinal mode at $\lambda_0 = 514.5$ nm wavelength. The laser power incident on the sample was 150 mW. Only *p*-polarized scattered light was examined for the purpose of selecting contributions coming only from the sagittal

0163-1829/95/51(15)/9875(6)/$06.00

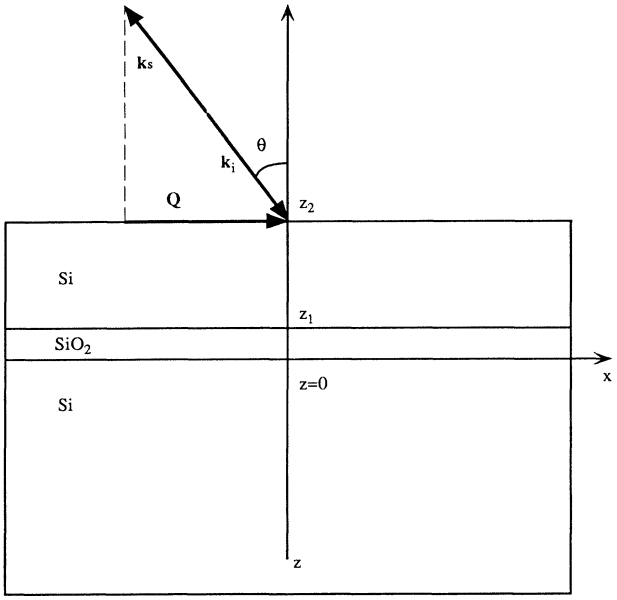

FIG. 1. Silicon on insulator structure: sample geometry and scattering configuration. The x axis is parallel to the surface phonon propagation wave vector, the z axis is normal to the surface. The origin of the z axis is taken at the SiO_2/Si interface.

modes. Spectra were taken at different angles of incidence, from 20° to 70°, in order to have different wave vector components parallel to the surface Q. In backscattering geometry $Q = (4\pi/\lambda_0)\sin\theta$, where θ is the angle of incidence.

The sample and scattering geometry is depicted in Fig. 1. The x axis is parallel to the phonon propagation wave vector, while the z axis is normal to the surface and points towards vacuum. The origin of the z axis is taken at the silica-substrate silicon interface.

To reduce the broadening caused by the finite collection aperture, a vertical slit ($\Delta\theta \approx \pm 2°$) was used in the collection. This slit avoids also the spurious splitting of Brillouin scattering peaks in the spectra, due to the interception of the backscattered photons by the mirror used to direct the incident light onto the sample.

III. RESULTS AND DISCUSSION

In Fig. 2(a), we present Brillouin spectra taken along the [100] direction for different angles of incidence. The velocity used in the horizontal axis is related to the experimental frequency shift Ω by the relationship $v = \Omega/Q$.

The experimental results are fairly well reproduced by the theoretical cross sections reported in Fig. 2(b). The computation of the p-p Brillouin cross section[6,8] takes into account both the elasto-optic and ripple contributions. In the calculations, literature data of the elastic, elasto-optic, and dielectric constants for Si and SiO_2 were assumed,[10] so that the theory does not contain any free parameter. Calculated cross sections were convoluted with a Gaussian curve in order to simulate the instrumental broadening. The Sezawa modes, present in the calculated acoustic spectra, give a negligible contribution to the scattered intensity. Although these modes couple to light through both the elasto-optic and ripple scattering mechanisms, they do not appear appreciably in the total cross section, due to destructive interference between these contributions, similarly to what happens in the case of SiO_2 films on a silicon substrate.[11] Therefore, all the spectra show only three significant structures, the low frequency peak due to the Rayleigh wave and two dominant peaks due to the pseudomodes.

In what follows, we will limit our discussion only to the pseudomodes. In order to analyze the relevant features, we performed measurements at different incidence angles for propagation along [100] and [110]. In these directions

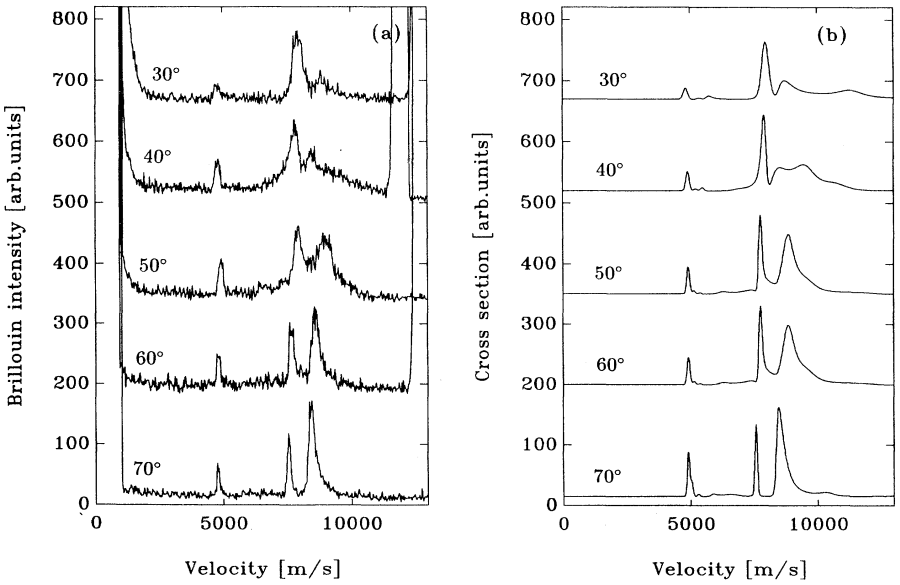

FIG. 2. (a) Anti-Stokes Brillouin spectra for different incidence angles taken along [100] in p-p polarization. (b) Theoretical cross sections evaluated at the same incidence angles. Data were convoluted with a Gaussian curve in order to simulate the instrumental broadening and were multiplied by an amplitude factor. No other free parameter was adopted.

and for the (001) surface, the sagittal waves decouple from the shear horizontal ones. The experimental velocity data are reported in Fig. 3 versus the surface wave vector Q and compared with the theoretical dispersion curves obtained by taking the velocity values corresponding to the maxima in the computed cross sections. The horizontal line represents the longitudinal threshold of silicon v_l.

For propagation along [100] the experimental velocity data of the higher energy pseudomode above v_l, labeled HL in the figure, have a nonmonotonic behavior and show an increase in velocity between $Q = 0.0157$ nm^{-1} and $Q = 0.0186$ nm^{-1} (corresponding to the range $40° - 50°$ for the incidence angle). This is explained by inspection of Fig. 2 and comparison with the calculated curves. In this interval of Q, a pseudomode from a higher branch of the continuum becomes visible. This pseudomode has a larger longitudinal polarization and, therefore, a greater elasto-optic scattering amplitude, as it will be explained later on.

In the case of [110] direction [Fig. 3(b)] for small values of Q, the dispersion relation exhibits a behavior similar to that of the [100] direction, but for Q greater than 0.017 nm^{-1}, a new branch lying below v_l, and labeled LL2 in the figure, appears. In order to analyze the relevant features of the observed pseudomodes it is necessary to discuss the behavior of the displacement fields. The Fourier component $\mathbf{w}(Q, \Omega, z)$ of the polarization field associated with surface acoustic phonons can be expanded as a sum of partial waves in each medium as

$$\mathbf{w}^{(i)}(Q, \Omega, z) = \sum_{\lambda=1}^{\Lambda(i)} e^{iq_\lambda^{(i)}(Q,\Omega)z} a_\lambda^{(i)}(Q, \Omega)\mathbf{e}_\lambda^{(i)}(Q, \Omega), \quad (1)$$

where Ω represents the surface phonon frequency. The index i indicates the medium (i=1 top silicon layer, i=2 silica layer, i=3 silicon substrate) and Λ is the number of partial waves entering Eq. (1). In each medium, $\mathbf{e}_\lambda^{(i)}(Q, \Omega)$ are the bulk eigenvectors and $q_\lambda^{(i)}(Q, \Omega)$ are the wave vector components perpendicular to the surface. The unknown coefficients $a_\lambda^{(i)}(Q, \Omega)$ are determined by imposing the acoustic boundary conditions[12] and are properly normalized.[8,13]

Since the velocity of the lower energy pseudomode, labeled LL in Fig. 3(a), is below v_l, its transverse component in silicon is represented by a traveling wave, whereas the longitudinal partial wave is evanescent. This fact may be appreciated in Fig. 4 where the square modulus of the displacement field associated with the pseudomode is shown for two different parallel wave vectors ($Q = 0.012$ nm^{-1} and $Q = 0.023$ nm^{-1}) along [100]. For both values of Q, the w_z component (full line) is very small while w_x (dashed line) is mainly confined in the silica layer. We remark that the phase velocity of this pseudomode is always higher than that of the medium in which it propagates and it is close to the velocity v_l of the Si matrix; nevertheless this pseudomode is strongly localized in SiO_2. The velocity slightly decreases as Q increases. The higher energy pseudomode, labeled HL in Fig. 3, lies above v_l, therefore all its partial components are traveling waves and lead to energy leakage into the bulk. The modal profiles, calculated for two different values of Q ($Q = 0.012$ nm^{-1} and $Q = 0.023$ nm^{-1}) and presented

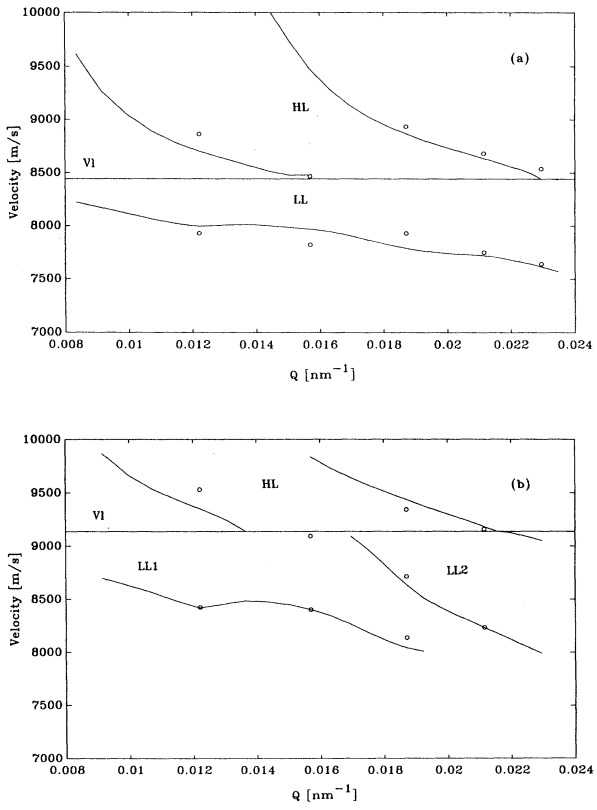

FIG. 3. Dispersion relations along [100] (a), and [110] (b) directions. Full lines represent theoretical curves obtained by taking the maxima positions in the cross sections. The horizontal line represents the longitudinal velocity (v_l) of silicon. We labeled with LL the pseudomodes, whose velocity is below v_l, and with HL those which are above v_l.

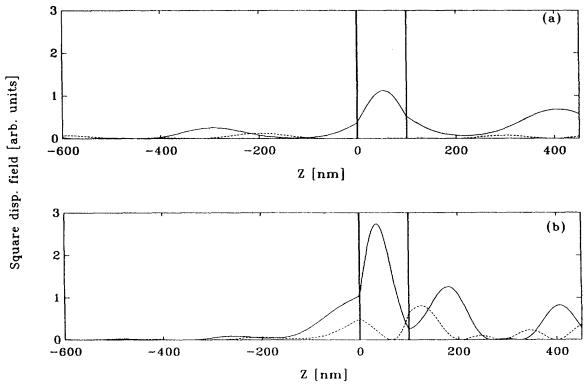

FIG. 4. Square modulus of the displacement field associated with the pseudomode LL observed in Fig. 3(a); (a) $Q = 0.012\,\text{nm}^{-1}$. (b) $Q = 0.023\,\text{nm}^{-1}$. Full line w_x, dashed line w_z. The vertical lines represent the interfaces. The z-axis origin is fixed at the substrate Si-SiO_2 interface.

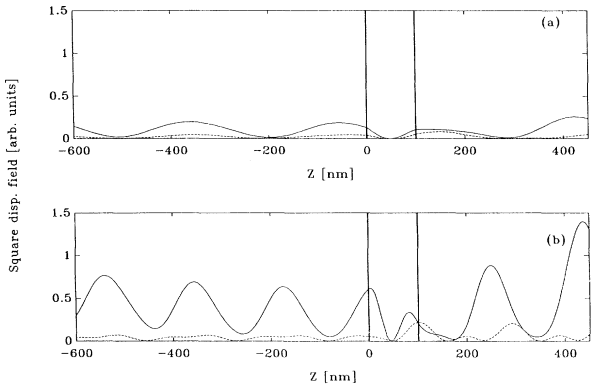

FIG. 5. Square modulus of the displacement field associated with the pseudomode HL observed in Fig. 3(a). The symbols and definitions are the same as in Fig. 4.

in Fig. 5, show that also this pseudomode is mainly longitudinally polarized; however, it is more localized in the top silicon layer than in SiO_2. This behavior is similar to that of the longitudinal resonance (LR) (Refs. 14–16) of a semi-infinite medium. As shown via numerical calculation by Byloos *et al.*,[8] when the silica layer thickness goes to zero both HL and LL approach the silicon LR. Therefore, the origin of these modes may be found in the modifications induced on the LR by the silica layer. When the SiO_2 thickness is above a critical value, the LR splits in two modes, the first one localized in silica, the second in the upper silicon. The degree of localization depends on the film thickness and on Q, as shown in Figs. 4 and 5.

We can now discuss the appearance of the branch below the longitudinal threshold of silicon observed in the dispersion relation for propagation along [110]. This will be accomplished by the analysis of the displacement profiles for both pseudomodes presented in Fig. 6 for

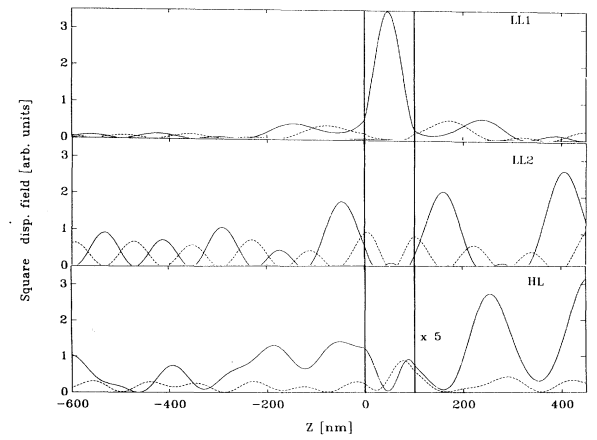

FIG. 6. Square modulus of the displacement field associated with the pseudomodes LL1, LL2, and HL observed in Fig. 3(b) for $Q = 0.018\,\mathrm{nm}^{-1}$; full line w_x, dashed line w_z. The vertical lines represent the interfaces. The z-axis origin is fixed at the substrate Si-SiO_2 interface.

$Q = 0.018\ \mathrm{nm}^{-1}$. The longitudinal component of the pseudomode LL1 is confined in the SiO_2 layer, where it presents no nodes, and goes to zero in silicon. On the contrary the pseudomode belonging to the new branch, labeled LL2, has some localization near the Si-SiO_2 interfaces and the leakage in the silica layer is large.

This feature is characteristic of bounded modes of increasing order like the guided sagittal modes of a single supported film (Rayleigh and Sezawa modes).[11] Therefore, by analogy, we might interpret LL1 as the first order mode and LL2 as the second order mode of the family of longitudinal guided pseudomodes in the silica layer. The behavior of the higher energy pseudomode, labeled HL in the figure, is similar to the corresponding one for the [100] direction.

The changes in localization of the pseudomodes will help us also to discuss the change in the relative intensity of HL, with respect to LL observed for propagation along [100], as a function of the incidence angle (Fig. 2). For these two peaks, which lie around the longitudinal threshold of silicon, only the elasto-optic mechanism is effective. The reason for this is that the coupling via ripple effect depends only on the component of the displacement field perpendicular to the surface.[7] As it may be seen in Fig. 4, the pseudomodes close to v_l have essentially longitudinal component, therefore, they give no ripple contribution. By numerical computation, we have verified that the main elasto-optic contribution comes from the top silicon layer. The mechanism of scattering in this case operates through two channels involving reflection of light from the first Si/SiO_2 interface (a detailed discussion of the mechanism of scattering is given in Ref. 8). In this case, the scattering amplitude is proportional to

$$k_{11}Q\sum_{\lambda} a_\lambda (e_\lambda)_x \left[e^{iq_\lambda z_2} - e^{iq_\lambda z_1}\right]/q_\lambda = ik_{11}Q\int_{z_1}^{z_2} dz\, w_x(z,\Omega), \tag{2}$$

where z_1 and z_2 are defined in Fig. 1 and k_{11} is the relevant elasto-optic constant of silicon. From Eq. (2), it can be seen that when the frequency approaches the longitudinal threshold v_l of silicon, the term with $q_\lambda = q_l \to 0$ becomes resonant and the cross section depends on the longitudinal component. Thus we conclude that, for the pseudomodes close to the longitudinal threshold, the visibility in the Brillouin spectrum depends on the localization of the longitudinal component in the upper Si layer.

In Fig. 2(a) for 70° incidence, the peak corresponding to the pseudomode HL is more intense than that corresponding to LL. When the incidence angle is decreased, this situation is going to be reversed and at 30° incidence LL has an intensity greater than HL. A qualitative explanation of this behavior can be given by referring to Fig. 4. It can be seen that, for the LL pseudomode, the longitudinal displacement component in the top silicon layer is larger when $Q \approx 0.0122\ \mathrm{nm}^{-1}$ [corresponding to the spectrum at 30° displayed in Fig. 2(a)] than when $Q \approx 0.0229\ \mathrm{nm}^{-1}$ (corresponding to 70° incidence). The HL pseudomode exhibits an opposite behavior, that is its

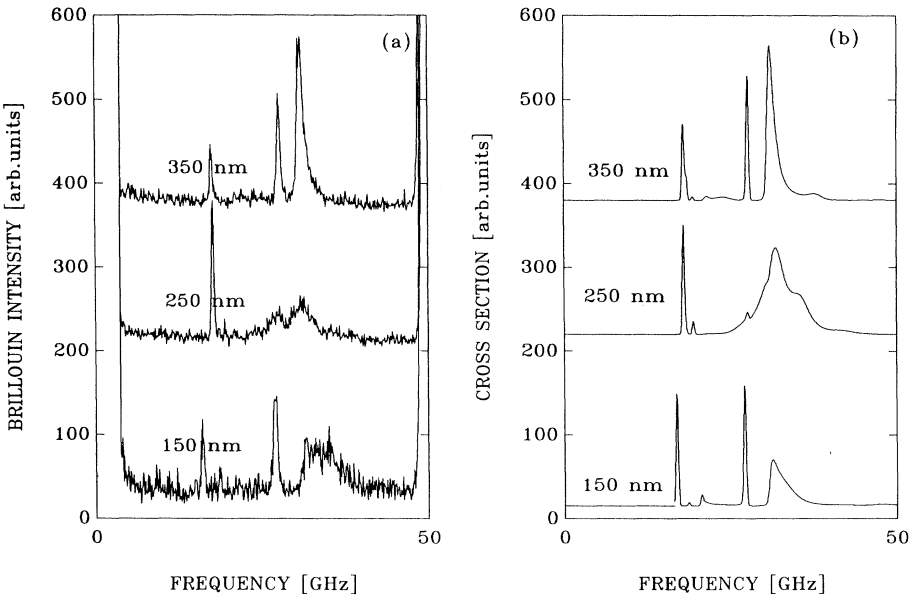

FIG. 7. Brillouin spectra along the [100] direction and calculated cross sections for an incidence angle of 70° for samples of different silicon layer thickness.

longitudinal component shows a higher localization in the silicon layer for higher angles [see Fig. 5(a) and Fig. 5(b)]. Since, as observed above, the scattering intensity depends on the magnitude of the longitudinal component in the top silicon layer, the different localization of the LL and HL pseudomodes explains the behavior of the Brillouin peaks with the incidence angle.

In Fig. 7 the Brillouin spectra of the samples, with different thicknesses of the top silicon layer (respectively, 150, 250, and 350 nm), taken at 70° incidence angle, are presented. The intensity of the peak below the longitudinal threshold depends strongly and in a nonmonotonic manner on the thickness of the Si layer.

While in the case of 350 nm and 150 nm the calculated cross sections of Fig. 7 resemble quite well the experimental spectra, differences are visible at 250 nm thickness. We found that the 250 nm case is a critical one where the calculated cross section strongly oscillates when the Si film thickness varies within ±5 nm around 250 nm. Since this uncertainty is of the order of the thickness inhomogeneities left after the removal of the Si layer by etching, the experimental spectra can be considered as an average of cross sections corresponding to different thicknesses. This could explain the differences with theory.

IV. CONCLUSIONS

Brillouin light scattering experiments in *p-p* polarization have been conducted on a Si/SiO_2 double layer on a silicon substrate. Longitudinally polarized pseudomodes have been detected and their dispersion relations for propagation along [100] and [110] have been determined. The experimental dispersion relations and the relative intensity of the peaks corresponding to longitudinal pseudomodes are discussed in terms of changes in localization by means of theoretical calculations.

The localization of the longitudinal component of the two pseudomodes observed below the longitudinal resonance of silicon for [110] propagation is analyzed. The different confinement of these pseudomodes has been utilized to interpret them as the first order and the second order modes of the family of longitudinal pseudomodes guided in the silica layer. A nonmonotonic behavior of the experimental Brillouin intensity with the thickness of the Si layer was observed.

ACKNOWLEDGMENTS

We gratefully acknowledge Dr. L. Meda and Dr. G. F. Cerofolini of Istituto Donegani, Novara, Italy for the supply of the samples and S. Bertoni of the same institute for the use of electron microscopy. Many thanks are due to Dr. M. Beghi, A. Gagliardi, and A. Mantegazza for their invaluable technical help. The present activity was funded by Progetto Finalizzato Materiali Speciali per Tecnologie Avanzate of Consiglio Nazionale delle Ricerche (C. E. Bottani, G. Ghislotti, P. Mutti) and by Ministero Università e Ricerca Scientifica e Tecnologica (C. Byloos, L. Giovannini, F. Nizzoli). C. Byloos and L. Giovannini have received financial support from the Istituto Nazionale Fisica della Materia.

* Also at Istituto Nazionale di Fisica della Materia, Unità di Ricerca Milano Politecnico, Milano, Italy.

[1] F. Nizzoli and J. R. Sandercock, in *Dynamical Properties of Solids,*, edited by G. K. Horton and A. A. Maradudin (Elsevier, Amsterdam, 1990), Vol. 6, p. 281.

[2] B. Hillebrands, S. Lee, G. I. Stegeman, H. Cheng, J. E. Potts, and F. Nizzoli, Phys. Rev. Lett. **60**, 832 (1988).

[3] G. Carlotti, D. Fioretto, L. Giovannini, G. Socino, V. Pelosin, and B. Rodmacq, Solid State Commun. **81**, 487 (1992).

[4] C. E. Bottani, G. Ghislotti, and P. Mutti, J. Phys. Condens. Matter **6**, L85 (1994).

[5] G. Ghislotti and C. E. Bottani, Phys. Rev. B **50**, 12 131 (1994).

[6] F. Nizzoli, C. Byloos, L. Giovannini, C. E. Bottani, G. Ghislotti, and P. Mutti, Phys. Rev. B **50**, 2027 (1994).

[7] R. Loudon, Phys. Rev. Lett. **40**, 581 (1978).

[8] C. Byloos, L. Giovannini, and F. Nizzoli, Phys. Rev. B **51**, 9867 (1995).

[9] J. R. Sandercock, Solid State Commun. **26**, 547 (1978).

[10] Si constants: ϵ=18.5 + 0.52i, c_{11}=166 GPa, c_{12}=63.9 GPa, c_{44}=79.6 GPa, k_{11}=53.2, k_{12}=25.0, k_{44}=23.4, ρ=2330 kg m^{-3}. SiO_2 constants: ϵ=2.16, c_{11}=78.5 GPa, c_{44}=31.2 GPa, k_{11}=0.55, k_{44}=0.345, ρ=2200 kg m^{-3}.

[11] V. Bortolani, G. Santoro, F. Nizzoli, and J. R. Sandercock, Phys. Rev. B **25**, 3442 (1982).

[12] G. W. Farnell and E. L. Adler, in *Physical Acoustics, Principles and Methods*, edited by W. P. Mason and R. N. Thurston (Academic Press, New York, 1972), Vol. IX, p. 109.

[13] V. Bortolani, A. M. Marvin, F. Nizzoli, and G. Santoro, J. Phys. C **16**, 1757 (1983).

[14] N.E. Glass and A.A. Maradudin, J. Appl. Phys. **54**, 796 (1983).

[15] R. E. Camley and F. Nizzoli, J. Phys. C **18**, 4795 (1985).

[16] G. Carlotti, D. Fioretto, L. Giovannini, F. Nizzoli, G. Socino, and L. Verdini, J. Phys. Condens. Matter **4**, 257 (1992).